RESEARCH ARTICLE

Chiral Supramolecular Organogel Constructed Using Riboflavin and Melamine: Its Application in Photo-Catalyzed Colorimetric Chiral Sensing and Enantioselective Adsorption

Marina Oka,[a] Ryo Kozako,[a] Yuta Teranishi,[a] Yuta Yamada,[a] Kazuhiro Miyake,[b] Takuya Fujimura,[a] Ryo Sasai,[a] Takahisa Ikeue,[a] Hiroki Iida*[a]

[a] M. Oka, R. Kozako, Y. Teranishi, Y. Yamada, Dr. T. Fujimura, Prof. Dr. R. Sasai, Prof. Dr. T. Ikeue, Prof. Dr. H. Iida
Department of Chemistry, Graduate School of Natural Science and Technology, Shimane University
1060 Nishikawatsu, Matsue 690-8504, Japan.
E-mail: iida@riko.shimane-u.ac.jp

[b] K. Miyake
Center for Material Research Platform, Nara Institute of Science and Technology (NAIST)
8916-5 Takayama, Ikoma, Nara 630-0192, Japan.

Supporting information for this article is given via a link at the end of the document.

Abstract: The synthesis of a chiral supramolecular organogel via the hierarchical helical self-assembly of optically active riboflavin and melamine derivatives is described herein. Owing to the photocatalysis of riboflavin and the supramolecular chirality induced in the helically stacked riboflavin/melamine complex, the gel is observed to act as a light-stimulated chiral sensor of optically active alcohols by detecting the change in color from yellow to green. The gel also served as an efficient chiral adsorbent, enabling optical resolution of a racemic compound with high chiral recognition ability.

Introduction

Helical supramolecular architectures with a controlled helix-sense, formed via self-assembly of small molecules, have garnered considerable research attention of late.[1] Constructing a controlled right- or left-handed helical array of small organic molecules that inherently possess functions like catalysis and optical property is a promising approach to creating novel chiral materials with attractive functions. Due to the induced and amplified supramolecular chirality, these helical supramolecules hold promise for applications like chiral discrimination and separation,[2] asymmetric catalysis,[3] circularly polarized luminescence,[4] and chiral optics and electronics.[5] However, their successful examples are limited compared to those of artificial helical polymers,[1c,6] and achieving a helical arrangement of the desired functional molecules in the supramolecular system remains challenging.

Riboflavin, commonly known as vitamin B_2, and its derivatives are ubiquitous in nature and participate in numerous biochemical processes by binding to proteins as cofactors.[7] For example, riboflavin acts as a blue-light-sensitive photoreceptor of phototropin, which regulates the phototropic responses of higher plants such as the bending of stems toward light. [8] Additionally, riboflavin acts as the catalytic active site of flavin-containing monooxygenases that are essential for xenobiotic detoxification.[9] Riboflavin consists of a planar π-conjugated isoalloxazine ring and a chiral ribityl group, which endow it with diverse properties including photosensitivity and optical, redox, and catalytic activities.[10] In addition, the sophisticated biological functions of flavoproteins and flavoenzymes are attributable to the well-designed chiral environment and noncovalent interactions with surrounding proteins. As evidenced by their diverse biological systems,[7-9] artificial chiral supramolecules with a helical array of riboflavin can be used as unique chiral materials with biomimetic or novel artificial properties. These findings are also important for the elucidation of the biological functions of the flavoproteins and flavoenzymes. Despite the remarkable progress achieved using the analogs of vitamin B_{12} such as porphyrins for the design of various functional supramolecular systems,[11] the development of riboflavin-containing supramolecules, and in particular, those with chiral functions such as chiral recognition ability and asymmetric catalysis has been scarcely conducted.[12]

Herein, we report a chiral supramolecular gel formed via the hierarchical helical self-assembly of riboflavin and melamine derivatives. The supramolecular gel with helically arranged riboflavin units exhibited a unique chiral recognition ability, enabling its application in the visible colorimetric chiral sensing of optically active analytes as well as the enantioselective adsorption of a chiral compound owing to its induced supramolecular chirality. The enantioselective color change of the gel is induced because of the photocatalysis of riboflavin; additionally, chiral sensing is triggered by light irradiation. Although several methods, including chiral high-performance liquid chromatography (HPLC), have been developed to accurately obtain chiral information, the development of simpler assays that can easily visualize chiral discrimination is a challenge.[13] Enantioselective sensors have also been demonstrated through the use of diverse chiral materials, including polymers,[14] supramolecules,[15] metal–organic frameworks,[16] and carbon nanotubes or graphene.[17] Colorimetric chiral detection based on the absorbance change for the chiral chromogenic unit is a promising method that facilitates unaided facile visual detection.[18]

Results and Discussion

The transparent supramolecular organogel was fabricated using a 2:1 mixture of carbamoylated riboflavin **F1**—prepared from riboflavin (vitamin B_2, Figure S1)—and N,N'-dioctyl melamine (**M**) in 1,2-dichloroethane (DCE). The gelation was completed by heating the mixture at 80 °C for 5 min, followed by cooling to 25 °C for 5 min (Figure 1A and Table S1).[19] The morphology of the supramolecular gel was characterized by scanning electron microscopy (SEM), scanning transmission electron microscopy (STEM), and atomic force microscopy (AFM); the results are shown in Figures 1B, S3, and S4. The SEM and STEM images of the diluted gel presented three-dimensional (3D) networks consisting of linearly extending fibrils, which are typical of helical macro- and supramolecules (Figures 1B and S3).[6b] Using AFM, nanofibers with an average height of 1.2 ± 0.2 nm arranged in a partially aligned parallel fashion were observed on the mica substrate (Figure S4). The magnified SEM images revealed that the fibrils had a helical structure, and the conformation was likely right-handed (Figures 1B and S3).

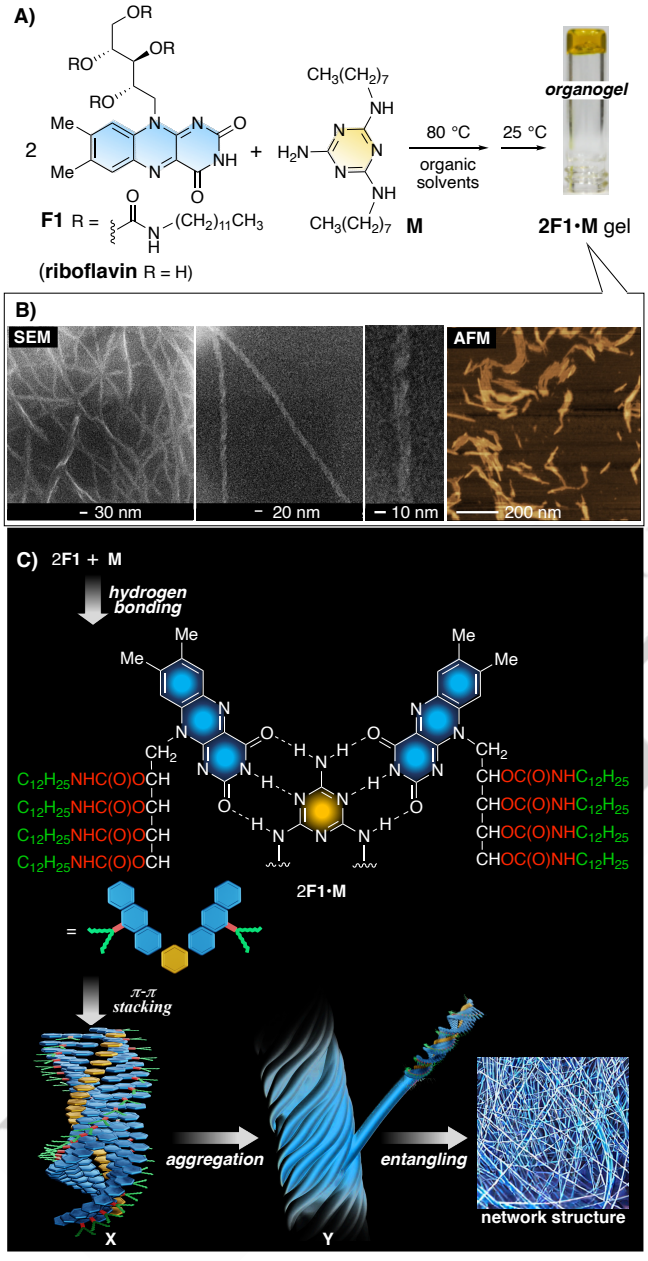

Figure 1. (A) Schematic of organogel formation using **F1** and **M**. The fabricated organogel is shown on the right. (B) SEM and AFM images of the supramolecular gel formed using **F1** and **M** in DCE (10 and 5.0 mM, respectively). (C) Schematic of the formation of helical nanofibers and the organogel through the hierarchical self-assembly of **F1** and **M**.

The proposed mechanism of the hierarchical self-assembly of **F1** and **M** is shown in Figure 1C. First, the complexation of two **F1** molecules with **M** (**2F1•M**) occurred via three-point hydrogen bonding between the C=O and N–H of the flavin ring and the N and N–H of melamine. Second, the **2F1•M** complexes with planar π-conjugated structures self-assembled to form a helically stacked supramolecular structure (**X**) with excess one-handedness. Despite the possible structural change caused by its adsorption onto the substrate surface, structure **X** might have corresponded to the fibrous structure, which had a height of ~1 nm, observed by AFM. Because the periphery of supramolecular helix **X** was covered by hydrophobic alkyl chains, the helix further aggregated to form supramolecular nanofibers (**Y**) with right-handed helical structures. The fibrillar nanostructures then entangled to construct a 3D-network structure that immobilized a large volume of solvents—the organogel.

To determine the supramolecular structure composed of **F1** and **M**, various spectroscopic analyses were performed. A job plot analysis of the ^{1}H NMR measurements of the **F1**/**M** mixture in $CDCl_3$ showed that two **F1** molecules were complexed with one **M** molecule (Figure S5).[20] The formation of three-point hydrogen bonds between **F1** and **M** was also confirmed by ^{1}H NMR and IR measurements (Supporting Information Section 4.5).[21,22] The conformation of the **2F1•M** complex (Figure 1C) was deduced using density functional theory calculations (Supporting Information Section 5).

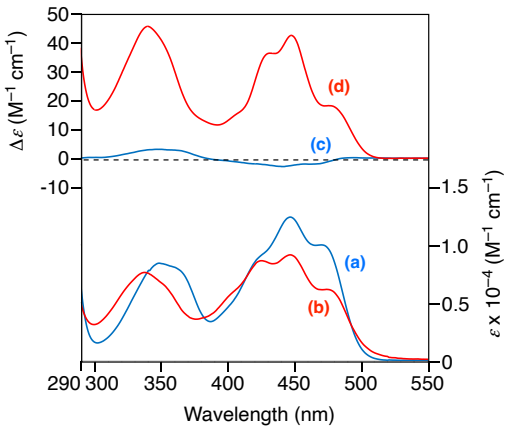

Figure 2. Absorption (a, b) and circular dichroism (CD) (c, d) spectra of **F1** (0.1 mM) in DCE (a, c) and a supramolecular gel formed by **F1** and **M** (10 and 5.0 mM, respectively) in DCE (b, d).

The CD and absorption spectra of the mixture of **F1** (10 mM) and **M** (5.0 mM) in DCE before and after gelation were analyzed to investigate the chiroptical properties of the compounds (Figure 2, Supporting Information Section 4.6). The DCE solution of **F1** showed characteristic absorption signals centered at approximately 350 and 450 nm that were attributed to the π-conjugated flavin chromophore. The absorption spectrum of the transparent yellow **2F1•M** gel revealed the hypochromic effect and blue-shift in the flavin chromophore regions, suggesting that the supramolecular structure was formed through the π-π stacking of the π-conjugated flavin ring.[23] The DCE solution of **F1** exhibited weak negative Cotton effects in these flavin chromophoric long-wavelength regions; however, the **2F1•M** gel displayed intense positive Cotton effects at approximately 450 nm. The CD spectral changes indicated that supramolecular chirality was induced and amplified through the self-assembly of **F1** and **M** by the chirality transfer from the optically active ribityl pendant of **F1**. The effect of the substituents of **F1** on the gelation ability was investigated using **F1** analogs, **F2**–**F5** (Figure S1). The carbamoyl moiety and long-chain dodecyl moiety introduced on the ribityl group of **F1** were essential for rapid gelation (Table S1 and Supporting Information Section 4.1). Therefore, supramolecular helix **X** (Figure 1C) was likely stabilized by i) the π–π stacking of the π-conjugated flavin and melamine rings, ii) the intermolecular hydrogen bonding of the carbamoyl units of **F1**, and iii) the solvophobic effect of the alkyl chains of the dodecyl carbamate of **F1**.

The applicability of the **2F1•M** supramolecular gel as a chiral material was verified. This enabled the straightforward colorimetric chiral discrimination of optically active compounds using visual detection based on color changes. Assuming that the **F1**/**M** mixture could detect the chirality of optically active analytes, supramolecular gels of **F1** and **M** (DCE, 10 and 5.0 mM, respectively) in the presence of (2*S*,3*S*)- and (2*R*,3*R*)-diethyl tartrate (**1**, 0.10 M) were prepared. The mixtures were placed in sample tubes sealed with caps to form yellow gels, which were then irradiated using visible light (blue LED, 7.2 W) for 4 h (Figure 3Aa). After 2 h of irradiation, the color of the gel containing (2*S*,3*S*)-**1** remained yellow, whereas that of the gel containing (2*R*,3*R*)-**1** turned green. This indicated that the chirality of **1** can be distinguished by the supramolecular assembly of **2F1•M**. We also performed enantioselective colorimetric sensing using other optically active alcohols **2** and **3** as the analytes (Figure 3Ab and c). This analysis showed that the addition of (*R*)-**2** and (2*R*,3*R*)-**3** preferentially results in a color change to green within 2 and 1 h, respectively.[24] By contrast, when optically active BINOL, 1-phenylethyl alcohol, and 1-phenylethyl amine were used as the analytes, the enantioselective color change was not observed (Figure S14). Based on the experiment using varying concentrations of **3**, the limit of detection for **3** that could be distinguished by the naked eye was estimated to be approximately 0.1 equiv (0.5 mM, Figure S15). The green color of the (*2R,3R*)-**3**-containing **2F1•M** gel was preserved for at least 72 h under N_2 atmosphere in the dark (Figure S16).

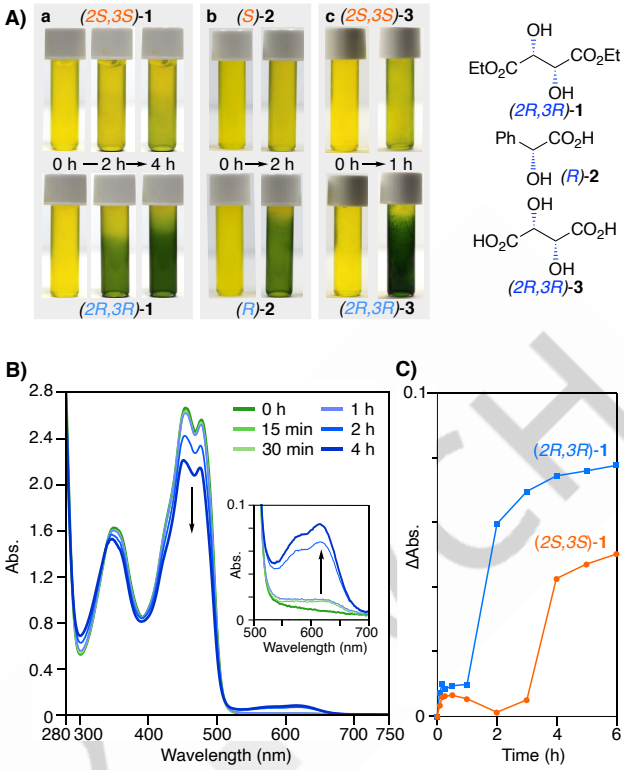

Figure 3. (A) Images of the **2F1•M** gels (5.0 mM) containing optically active **1** (20 equiv in DCE), **2** (2.0 equiv in DCE), and **3** (2.0 equiv in DCE/MeOH (98:2 v/v)) in sample tubes (0.8 mL). The length of time of the color change is also shown. (B) Absorption spectra of the **2F1•M** gel (DCE, 1.0 mM) containing (2*R*,3*R*)-**1** (20 equiv) in a 1 mm quartz cell upon light irradiation (blue LED, 7.2 W) and an enlarged view of the longer-wavelength region (inset). (C) The change in absorption intensity of the peak at 620 nm.

The change in the absorption spectra during irradiation of the (2*R*,3*R*)-**1**-containing gel is shown in Figure 3B. Upon exposure to light, the characteristic absorption peak at ~450 nm arising from the conjugated flavin ring of **F1** gradually weakened, while the gel gave rise to a new absorption signal centered at 620 nm, causing the dark green color. The appearance of the new species with the absorption signal in the longer-wavelength region was attributed to the generation of the flavin radical (**F1H**$^{\bullet}$, Scheme 1).[25] The electron spin resonance (ESR) analysis of the green-colored (*R*)-**2**-containing gel obtained after light irradiation revealed an apparent radical signal with a *g*-value of 2.0041, indicating the formation of radical flavin **F1H**$^{\bullet}$ (Figure S17a).[25b] Figure 3D presents the change in absorption intensity of the peak at 620 nm for the **2F1•M** gels containing 20 equiv of (2*R*,3*R*)- or (2*S*,3*S*)-**1** (Figure S11). The color change was not continuous but drastically increased in intensity after a specific induction period. The 620 nm absorption peak of the gel containing (2*R*,3*R*)-**1** began increasing after 1 h of light irradiation. However, the absorption increased after ~3 h in the gel containing (2*S*,3*S*)-**1**. Because of the unusual nonlinear absorption change, a distinct color change can be easily recognized (Figure 3A). Furthermore, the light-responsive nature of the complex means that the changed or unchanged color can be preserved by terminating the

light irradiation. The present gel is unique because it promotes colorimetric chiral sensing via light irradiation regulation.[26]

The mechanism underlying the light-responsive color change of the supramolecular gel containing chiral alcohol is proposed in Scheme 1. Riboflavin derivatives are known to act as photocatalysts,[27] and they efficiently promote the photooxidation of alcohols to form aldehydes, ketones, and carboxylic acids upon light irradiation.[28] The visible light irradiation of yellow **F1** generates excited ^{3}**F1***, which has strong oxidizing power. This facilitates the oxidation of alcohols, producing the corresponding ketones and green-colored flavin radical (**F1H**$^\bullet$).[25c,28c,29] **F1H**$^\bullet$ exists at the equilibrium between proportionation and disproportionation, forming yellow **F1** and almost colorless **F1H$_2$**.[25a,b] Under aerobic conditions, **F1H**$^\bullet$ and **F1H$_2$** react with molecular oxygen (O_2) to form **F1**.[25a,b] However, the sample tube was filled with the supramolecular gel and sealed with a screw cap to prevent contact with air (O_2). Therefore, **F1H**$^\bullet$ generated by the photooxidation of alcohols was initially converted to **F1** by reacting with the O_2 remaining in the gel. After the consumption of the O_2 dissolved in the gel, **F1H**$^\bullet$ accumulated, and the gel gradually turned green. This mechanism explains the induction period observed in Figure 3C. Therefore, decreasing the amount of dissolved O_2 in the gel is expected to shorten the induction period and response time of the color change. The **2F1•M** gel was chiral, resulting in different reaction rates for each alcohol enantiomer. Generally, continuous color changes are difficult to distinguish. However, the reverse reaction pathway from **F1H**$^\bullet$ to **F1** in this system resulted in a significant difference in a quantity of **F1H**$^\bullet$ present at a certain time, such that the gel containing the enantiomer that preferentially reacts showed a marked color change. The structural change of the **2F1•M** gel (5.0 mM) containing (*2R,3R*)-**1** (20 equiv) was observed via TEM; the 3D network structure comprising nanofibrils was not significantly changed before and after the color change induced by light irradiation (Figure S18). As indicated by the change in the absorption spectra (Figure 3B), the color change seems to result from the partial conversion of **F1** to **F1H**· radicals, instead of from the changes in the higher-order structure.

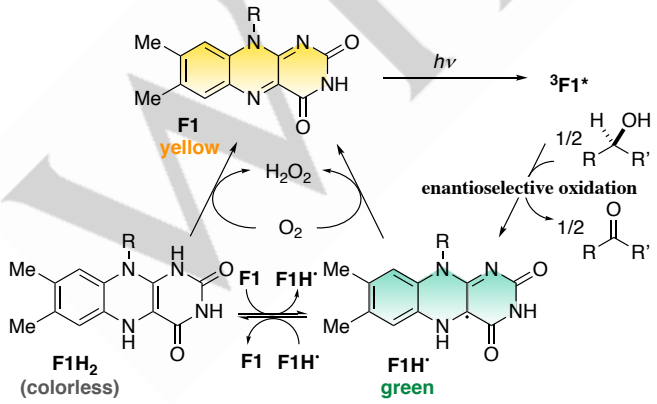

Scheme 1. Proposed catalytic cycle for the photooxidation of chiral alcohols.

The chiral recognition ability of the **2F1•M** gel was characterized by enantioselective adsorption experiments (Figure 4).[30] We prepared a xerogel by drying the **2F1•M** organogel of DCE in vacuo, and then allowed it to stand in an acetonitrile solution of racemic BINOL (*rac*-**4**) for 24 h. Therefore, the xerogel of **2F1•M** was preferentially adsorbed (*S*)-**4** with 46% enantiomeric excess (ee) (Figure 4A). Based on the quantity and ee value of adsorbed **4**, the separation factor (α),[30a,b] which is an index used in chiral HPLC to evaluate the chiral resolving ability of chiral stationary phases, was calculated as 5.11. This remarkably high α value indicates that this xerogel can function as a practical chiral recognition material, particularly as the chiral stationary phase (CSP) in chiral HPLC for complete separation of enantiomers.[31] The xerogel collected after the enantioselective adsorption experiment of *rac*-**4** could be utilized again, and it could enantioselectively adsorb (*S*)-**4** with 42% ee (Figure 4A). The separation factor of the second run decreased slightly compared to that of the first run (α = 5.11) but was still sufficiently high for efficient chiral separation.[31] Compared with the xerogel, the 2:1 mixture of **F1** and **M** before gelation adsorbed (*R*)-**4** with 4.1% ee (α = 1.10) (Figure 4B). The reversal of stereoselectivity and significant increase in the α value after gelation indicated that the supramolecular chirality induced in the supramolecular architecture of **F1** and **M** played a crucial role in chiral recognition.

We also attempted the enantioselective adsorption of other analytes using the **2F1•M** organogel of DCE (Table 1). To our delight, when an acetonitrile solution of the racemic analysts was

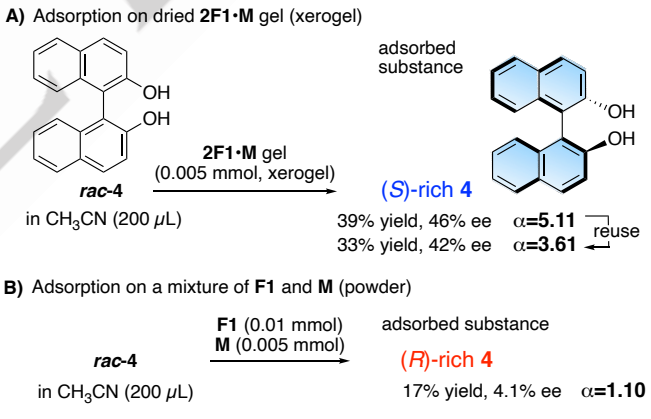

Figure 4. Enantioselective adsorption of *rac*-**4** on (A) a dried **2F1•M** gel (xerogel) and (B) a 2:1 mixture of **F1** and **M** before gelation (powder). The yields and ees of adsorbed **4** were averaged over three runs.

Table 1: Eanantioselective adsorption of racemic analytes **5**-**7** using **2F1•M** organogel as a chiral adsorbent.[a]

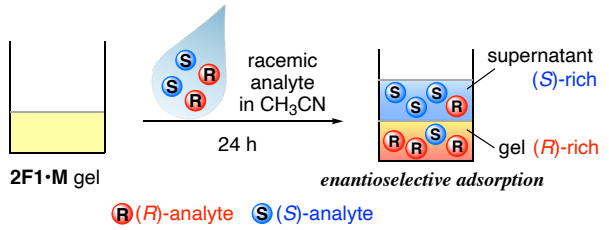

Entry	Analyte	Yield of Adsorbed Analyte [%]	Ee of Adsorbed Analyte [%]	Separation Factor [α][b]
1	**5**	7.19	55.7 (*R*)	3.97 (±0.84)
2	**6**	22.8	5.39 (*S*)	1.21 (±0.056)
3	**7**	19.3	16.3 (*S*)	1.51 (±0.092)

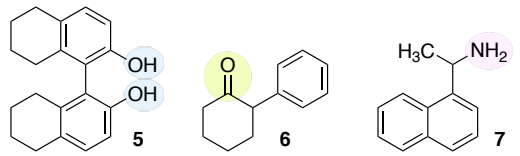

[a]Determined by chiral HPLC analysis of the supernatant solution. All values are the average of the results of four consecutive runs. [b]Calculated according to the equation $\alpha = (F_{major}\ (\%)/F_{minor}\ (\%))/(A_{major}\ (\%)/A_{minor}\ (\%))$, where F_{major} and F_{minor} are the percentages of major and minor enantiomers, respectively, of the free analyte in the supernatant solutions, and A_{major} and A_{minor} are the percentages of the major and minor enantiomers of adsorbed analyte, respectively. Values in parentheses are standard deviations.

added onto the **2F1•M** organogel and allowed to stand for 24 h, the gel adsorbed one of the enantiomers enantioselectively. The BINOL analogue (*R*)-**5** was enantioselectively adsorbed on the gel, yielding a remarkably high α value of 3.97 (entry 1). In addition to the alcohols, the **2F1•M** organogel demonstrated apparent chiral recognition ability towards chiral ketone **6** and amine **7**, and selectively adsorbed (*S*)-**6** and (*S*)-**7** with α values of 1.21 and 1.51, respectively (entries 2 and 3). The detailed mechanism of this process is not clear at this stage, but the hydrogen-bonding interactions among the hydroxy, carbonyl, and amino groups of **4**–**7** and the helically arranged carbamoyl unit of **F1** likely contribute to efficient chiral recognition.

Conclusion

A novel riboflavin/melamine-based chiral supramolecular gel was developed, and it enabled the light-stimulated colorimetric chiral discrimination and enantioselective adsorption of chiral alcohols, ketones, and amines. The chiral recognition ability was derived from the supramolecular chirality which was likely induced by the hierarchical self-assembly of riboflavin and melamine derivatives. To the best of our knowledge, this is the first reported example of helical supramolecular assembly enabling chiral photo-organocatalysis and efficient enantioselective adsorption. This finding can be used to develop novel bioinspired chiral supramolecular architectures and soft materials with favorable functions.

Supporting Information

Experimental details and procedures; supplemental Figures and Tables; spectroscopic, microscopic, and HPLC data; DFT calculation (PDF). The authors have cited additional references within the Supporting Information.[32-35]

Acknowledgements

The SEM and STEM measurements were conducted in Nara Institute of Science and Technology (NAIST), supported by the Nanotechnology Platform Program (Synthesis of Molecules and Materials) of the Ministry of Education, Culture, Sports, Science and Technology (MEXT), Japan (JPMXP09S19NR0033). The authors thank Prof. Tsuyoshi Kawai and Prof. Yo Shimizu (NAIST) for their help and advice with SEM and STEM. The authors acknowledge support from Prof. Takayuki Tanaka of Kyoto University for the ESR measurement. The CD analysis was performed at the Interdisciplinary Center for Science Research, Shimane University. The authors also thank Prof. Yasushi Imada and Prof. Keiji Minagawa (Tokushima University) for their help with the rheological property measurements. This work was supported in part by JSPS/MEXT KAKENHI (Grant-in-Aid for Scientific Research (C), 19K05617), Takahashi Industrial and Economic Research Foundation, Kumagai Foundation for Science & Technology, and Iketani Science and Technology Foundation. MO is grateful for the Grant-in-Aid for JSPS Fellows (23KJ1600) and JST SPRING (JPMJSP2155).

Conflict of interest

The authors declare no conflict of interest.

Data availability statement

The data that support the findings of this study are available in the supplementary material of this article.

Keywords: self-assembly • gels • chiral sensing • optical resolution • riboflavin

[1] a) A. R. A. Palmans, E. W. Meijer, *Angew. Chem., Int. Ed.* **2007**, *46*, 8948-8968; b) M. H. Liu, L. Zhang, T. Y. Wang, *Chem. Rev.* **2015**, *115*, 7304-7397; c) E. Yashima, N. Ousaka, D. Taura, K. Shimomura, T. Ikai, K. Maeda, *Chem. Rev.* **2016**, *116*, 13752-13990; d) P. Y. Xing, Y. L. Zhao, *Acc. Chem. Res.* **2018**, *51*, 2324-2334.

[2] a) K. Kodama, Y. Kobayashi, K. Saigo, *Chem. – Eur. J.* **2007**, *13*, 2144-2152; b) X. Chen, Z. Huang, S.-Y. Chen, K. Li, X.-Q. Yu, L. Pu, *J. Am. Chem. Soc.* **2010**, *132*, 7297-7299; c) T. Tu, W. Fang, X. Bao, X. Li, K. H. Doetz, *Angew. Chem., Int. Ed.* **2011**, *50*, 6601-6605; d) J. Jung, S.-J. Moon, J. Ahn, J. Jaworski, S. Shinkai, *ACS nano* **2013**, *7*; e) X. F. Wang, P. F. Duan, M. H. Liu, *Chem.- Asian J.* **2014**, *9*, 770-778; f) K. Salikolimi, V. K. Praveen, A. A. Sudhakar, K. Yamada, N. N. Horimoto, Y. Ishida, *Nat. Commun.* **2020**, *11*.

[3] a) Q. Jin, L. Zhang, H. Cao, T. Wang, X. Zhu, J. Jiang, M. Liu, *Langmuir* **2011**, *27*, 13847-13853; b) M. Raynal, F. Portier, P. W. N. M. van Leeuwen, L. Bouteiller, *J. Am. Chem. Soc.* **2013**, *135*, 17687-17690; c)

E. Huerta , B. van Genabeek , B. A. G. Lamers, M. M. E. Koenigs, E. W. Meijer, A. R. A. Palmans, *Chem. –Eur. J.* **2015**, *21*, 3682-3690; d) A. Desmarchelier, X. Caumes, M. Raynal, A. Vidal-Ferran, P. van Leeuwen, L. Bouteiller, *J. Am. Chem. Soc.* **2016**, *138*, 4908-4916; e) J. Jiang, Y. Meng, L. Zhang, M. Liu, *J. Am. Chem. Soc.* **2016**, *138*, 15629-15635; f) Z. C. Shen, Y. T. Sang, T. Y. Wang, J. Jiang, Y. Meng, Y. Q. Jiang, K. Okuro, T. Aida, M. H. Liu, *Nat. Commun.* **2019**, *10*.

[4] a) T. Kaseyama, S. Furumi, X. Zhang, K. Tanaka, M. Takeuchi, *Angew. Chem., Int. Ed.* **2011**, *50*, 3684-3687; b) J. Z. Liu, H. M. Su, L. M. Meng, Y. H. Zhao, C. M. Deng, J. C. Y. Ng, P. Lu, M. Faisal, J. W. Y. Lam, X. H. Huang, H. K. Wu, K. S. Wong, B. Z. Tang, *Chem. Sci.* **2012**, *3*, 2737-2747; c) J. Kumar, T. Nakashima, H. Tsumatori, M. Mori, M. Naito, T. Kawai, *Chem. –Eur. J.* **2013**, *19*, 14090-14097; d) D. Yang, P. F. Duan, L. Zhang, M. H. Liu, *Nat. Commun.* **2017**, *8*; e) S. Hu, L. Hu, X. Zhu, Y. Wang, M. Liu, *Angew. Chem., Int. Ed.* **2021**, *60*, 19451-19457

[5] a) X. Feng, V. Marcon, W. Pisula, M. R. Hansen, J. Kirkpatrick, F. Grozema, D. Andrienko, K. Kremer, K. Muellen, *Nat. Mater.* **2009**, *8*, 421-426; b) Y. Zhang, P. Chen, L. Jiang, W. Hu, M. Liu, *J. Am. Chem. Soc.* **2009**, *131*, 2756-2757.

[6] a) T. Nakano, Y. Okamoto, *Chem. Rev.* **2001**, *101*, 4013-4038; b) E. Yashima, K. Maeda, H. Iida, Y. Furusho, K. Nagai, *Chem. Rev.* **2009,** *109*, 6102-6211; c) R. P. Megens, G. Roelfes, *Chem. – Eur. J.* **2011**, *17*, 8514-8523; d) T. Leigh, P. Fernandez-Trillo, *Nat. Rev. Chem.* **2020**, *4*, 291-310; e) L. Zhou, K. He, N. Liu, Z. Q. Wu, *Polym. Chem.* **2022**, *13*, 3967-3974.

[7] a) F. Müller, *Chemistry and Biochemistry of Flavoenzymes*. CRC Press: Boston, **1991**; b) V. Massey, *Biochem. Soc. Trans* **2000,** *28*, 283-296; c) E. Silva, A. M. Edwards, *Flavins: Photochemistry and Photobiology*. Royal Society of Chemistry: Cambridge, **2006**; d) S. Weber, E. Schleicher, *Flavins and Flavoproteins Methods and Protocols*. Springer Humana: New York, **2014**.

[8] a) W. R. Briggs, J. M. Christie, *Trends Plant Sci.* **2002,** *7*, 204-210; b) J. Christie, *Annu. Rev. Plant Biol.* **2007,** *58*, 21-45.

[9] a) W. J. H. van Berkel, N. M. Kamerbeek, M. W. Fraaije, *J. Biotechnol.* **2006,** *124* (4), 670-689; b) C. T. Walsh, T. A. Wencewicz, *Nat. Prod. Rep.* **2013,** *30*, 175-200; c) G. Bailleul, G. Yang, C. R. Nicoll, A. Mattevi, M. W. Fraaije, M. L. Mascotti, *Nat. Commun.* **2023,** *14*, 1042.

[10] Riboflavin appears to be complex, but, is a sustainable functional molecule that is inexpensive ($20–30/kg, 80% grade for animal feed) and available in large quantities (~9 kt/year, in 2015) owing to its production from plant resources such as vegetable oils, starch hydrolysates, and corn steep liquor via biological fermentation. a) S. K. Schwechheimer, E. Y. Park, J. L. Revuelta, J. Becker, C. Wittmann, *Appl. Microbiol. Biotechnol.* **2016,** *100*, 2107-2119; b) L. A. Averianova, L. A. Balabanova, O. M. Son, A. B. Podvolotskaya, L. A. Tekutyeva, *Front. Bioeng. Biotechnol.* **2020,** *8*, 570828.

[11] a) I. Beletskaya, V. S. Tyurin, A. Y. Tsivadze, R. Guilard, C. Stern, *Chem. Rev.* **2009,** *109*, 1659-1713; b) *Porphyrin-based Supramolecular Architectures: From Hierarchy to Functions*. ed. S. Ma, and G. Verma, The Royal Society of Chemistry: **2021**; c) H. S. W. Lee, H. Park, D. Ryu, W. D. Jang, *Chem. Soc. Rev.* **2023,** *52*, 1947-1974.

[12] For examples of riboflavin-containing supramolecules with chiral functions, see a) S.-Y. Ju, J. Doll, I. Sharma, F. Papadimitrakopoulos, *Nature Nanotech.* **2008,** *3*, 356-362; b) H. Iida, S. Iwahana, T. Mizoguchi, E. Yashima, *J. Am. Chem. Soc.* **2012,** *134*, 15103-15113; c) H. Iida, M. Miki, S. Iwahana, E. Yashima, *Chem. –Eur. J.* **2014,** *20*, 4257-4262.

[13] a) K. Busch, M. Busch, *Chiral Analysis*. Elsevier: **2006**; b) D. Leung, S. O. Kang, E. V. Anslyn, *Chem. Soc. Rev.* **2012,** *41*, 448-479; c) X. Zhang, J. Yin, J. Yoon, *Chem. Rev.* **2014,** *114*, 4918-4959.

[14] a) L. Torsi, G. M. Farinola, F. Marinelli, M. C. Tanese, O. H. Omar, L. Valli, F. Babudri, F. Palmisano, P. G. Zambonin, F. Naso, *Nat. Mater* **2008**, *7*, 412-417; b) J. G. Ibanez, M. E. Rincón, S. Gutierrez-Granados, M. h. Chahma, O. A. Jaramillo-Quintero, B. A. Frontana-Uribe, *Chem. Rev.* **2018**, *118*, 4731-4816.

[15] a) G. A. Hembury, V. V. Borovkov, Y. Inoue, *Chem. Rev.* **2008**, *108*, 1-73; b) L. J. Chen, H. B. Yang, M. Shionoya, *Chem. Soc. Rev.* **2017**, *46*, 2555-2576.

[16] a) K. Zhan, Y. Jiang, L. Heinke, *Chem. Commun.* **2023**, *59*, 8704-8707; b) S. Okur, P. Qin, A. Chandresh, C. Li, Z. Zhang, U. Lemmer, L. Heinke, *Angew. Chem. Int. Ed.* **2021**, *60*, 3566-3571.

[17] a) N. J. Kybert, M. B. Lerner, J. S. Yodh, G. Preti, A. T. C. Johnson, *ACS Nano* **2013**, *7*, 2800-2807; b) Y. Zhang, X. Liu, S. Qiu, Q. Zhang, W. Tang, H. Liu, Y. Guo, Y. Ma, X. Guo, Y. Liu, *J. Am. Chem. Soc.* **2019**, *141*, 14643-14649.

[18] a) Y. Kubo, S. y. Maeda, S. Tokita, M. Kubo, *Nature* **1996,** *382*, 522-524; b) K. Tsubaki, M. Nuruzzaman, T. Kusumoto, N. Hayashi, W. Bin-Gui, K. Fuji, *Org. Lett.* **2001,** *3*, 4071-4073; c) R. Eelkema, R. A. van Delden, B. L. Feringa, *Angew. Chem., Int. Ed.* **2004,** *43*, 5013-5016; d) J. F. Folmer-Andersen, V. M. Lynch, E. V. Anslyn, *J. Am. Chem. Soc,* **2005,** *127*, 7986-7987; e) K. Tsubaki, D. Tanima, M. Nuruzzaman, T. Kusumoto, K. Fuji, T. Kawabata, *J. Org. Chem.* **2005,** *70*, 4609-4616; f) J. H. Jung, S. J. Lee, J. S. Kim, W. S. Lee, Y. Sakata, T. Kaneda, *Org. Lett.* **2006,** *8*, 3009-3012; g) K. Maeda, H. Mochizuki, M. Watanabe, E. Yashima, *J. Am. Chem. Soc.* **2006,** *128*, 7639-7650; h) D. Leung, J. F. Folmer-Andersen, V. M. Lynch, E. V. Anslyn, *J. Am. Chem. Soc.* **2008,** *130*, 12318-12327; i) H. E. Lee, H. Y. Ahn, J. Mun, Y. Y. Lee, M. Kim, N. H. Cho, K. Chang, W. S. Kim, J. Rho, K. T. Nam, *Nature* **2018,** *556*, 360-365; j) K. Maeda, D. Hirose, M. Nozaki, Y. Shimizu, T. Mori, K. Yamanaka, K. Ogino, T. Nishimura, T. Taniguchi, M. Moro, E. Yashima, *Sci. Adv.* **2021,** *7*, eabg5381.

[19] The obtained supramolecular gel was fragile and sensitive to mechanical perturbation. Rheological property measurements of the organogel revealed viscoelastic behavior; *i.e.*, storage modulus larger than loss modulus (G' >> G'')—a phenomenon typically observed for gels (Figure S2). G. M. Kavanagh, S. B. Ross-Murphy, *Prog. Polym. Sci.* **1998,** *23*, 533-562.

[20] To prevent the rapid gelation, which could lead to the disappearance of the NMR signals during the measurement due to the anisotropic effect, the ^{1}H NMR measurement was conducted in $CDCl_3$, which is less prone to gel formation (Table S1).

[21] The imide moiety of flavins is known to form three-point hydrogen bonding with 2,6-diaminopyridines. a) N. Tamura, K. Mitsui, T. Nabeshima, Y. Yano, *J. Chem. Soc., Perkin Trans. 2* **1994**, 2229-2237; b) E. Breinlinger, A. Niemz, V. M. Rotello, *J. Am. Chem. Soc.* **1995,** *117*, 5379-5380; c) G. Cooke, *Angew. Chem., Int. Ed.* **2003,** *42*, 4860-4870; d) V. Nandwana, I. Samuel, G. Cooke, V. M. Rotello, *Acc. Chem. Res.* **2013,** *46*, 1000-1009.

[22] In aqueous medium, non-substituted riboflavin and melamine forms the supramolecular complex in a mole ratio of 3:1 through the multiple hydrogen bonding, thus results in hydrogel. a) S. Manna, A. Saha, A. K. Nandi, *Chem. Commun.* **2006**, 4285-4287; b) A. Saha, S. Manna, A. K. Nandi, *Langmuir* **2007,** *23*, 13126-13135; c) J. Bachl, A. Hohenleutner, B. B. Dhar, C. Cativiela, U. Maitra, B. König, D. D. Diaz, *J. Mater. Chem. A* **2013,** *1*, 4577-4588.

[23] The flavin rings are known to form π-π stacking in solution and solid phases. a) M. Ebitani, Y. In, T. Ishida, K. Sakaguchi, J. L. Flippen-Anderson, I. L. Karle, *Acta Crystallogr., Sect. B: Struct. Sci.* **1993,** *B49*, 136-144; b) H. Nakade, B. J. Jordan, H. Xu, G. Han, S. Srivastava, R. R. Arvizo, G. Cooke, V. M. Rotello, *J. Am. Chem. Soc.* **2006,** *128*, 14924-

14929; c) H. Iida, T. Mizoguchi, S.-D. Oh, E. Yashima, *Polym. Chem.* **2010,** *1*, 841-848.

[24] By the light-irradiation, the greenish yellow fluorescence of the gel, originated from **F1**, was gradually quenched, but the rate of quenching also depended on the stereochemistry of the chiral analyte (Figure S13).

[25] a) C. Kemal, T. W. Chan, T. C. Bruice, *J. Am. Chem. Soc.* **1977,** *99*, 7272-7286; b) E. J. Nanni, Jr., D. T. Sawyer, S. S. Ball, T. C. Bruice, *J. Am. Chem. Soc.* **1981,** *103*, 2797-2802; c) U. Megerle, M. Wenninger, R. J. Kutta, R. Lechner, B. König, B. Dick, E. Riedle, *Phys. Chem. Chem. Phys.* **2011,** *13*, 8869-8880.

[26] Due to the controllable nature of light, the photo-responsive sensory materials are expected to allow the synchronized initiation of multiple measurements by light ON/OFF switching and allow for the preservation of the change at a desired stage. a) D. H. Qu, Q. C. Wang, Q. W. Zhang, X. Ma, H. Tian, *Chem. Rev.* **2015,** *115*, 7543-7588; b) F. Xu, B. L. Feringa, *Adv. Mater.* **2023**, 35, 2204413.

[27] a) B. König, S. Kümmel, E. Svobodová, R. Cibulka, *Phys. Sci. Rev.* **2018,** *3*, 20170168; b) B. Cheng, B. König in *Flavin-Based Catalysis*, (Eds.: R. Cibulka, M. W. Fraaije), Wiley-VCH: Weinheim, **2021**; pp 245-264; c) E. Svobodová, R. Cibulka in *Flavin-Based Catalysis*, (Eds.: R. Cibulka, M. W. Fraaije), Wiley-VCH: Weinheim, **2021**; pp 265-291.

[28] For examples of photo-catalyzed alcohol oxidations, see: a) S. Fukuzumi, S. Kuroda, T. Tanaka, *J. Am. Chem. Soc.* **1985,** *107*, 3020-3027; b) R. Cibulka, R. Vasold, B. König, *Chem .-Eur. J.* **2004,** *10*, 6223-6231; c) C. Feldmeier, H. Bartling, K. Magerl, R. M. Gschwind, *Angew. Chem., Int. Ed.* **2015,** *54*, 1347-1351, and refs 25c and 27a. Also see the pioneering example of flavin-based gel catalyst for photooxidation of alcohols.[22c]

[29] It is not clear whether the present photooxidation by **F1** proceeds by a one- or two-electron transfer process.[28c] In the latter case, $\mathbf{F1H_2}$ directly formed by the alcohol oxidation is converted to $\mathbf{F1H^{\bullet}}$ by reacting with **F1** through the proportionation process.

[30] a) E. Yashima, J. Noguchi, Y. Okamoto, *Macromolecules* **1995,** *28*, 8368-8374; b) E. Anger, H. Iida, T. Yamaguchi, K. Hayashi, D. Kumano, J. Crassous, N. Vanthuyne, C. Roussel, E. Yashima, *Polym. Chem.* **2014,** *5*, 4909-4914; c) Y. W. Peng, T. F. Gong, K. Zhang, X. C. Lin, Y. Liu, J. W. Jiang, Y. Cui, *Nat. Commun.* **2014,** *5*, 4406.

[31] A separation factor in the range of 1.2–1.3 is frequently observed for the successful CSPs for chiral HPLC, which is sufficiently high for complete chiral separation of enantiomers. a) Y. Okamoto, T. Nakano, *Chem. Rev.* **1994,** *94*, 349-372; b) Y. Okamoto, E. Yashima, *Angew. Chem., Int. Ed.* **1998,** *37*, 1020-1043; c) E. Yashima, H. Iida, Y. Okamoto, *Top. Curr. Chem.* **2013,** *340*, 41-72.

[32] J. Xu, G. Wu, Z.Wang, X. Zhang, *Chem. Sci.*, **2012**, *3*, 3227-3230.

[33] Y. C. Charalambides, S. C. Moratti, *Synth. Commun.*, **2007**, *37*, 1037-1044.

[34] T. Sakai, T. Kumoi, T. Ishikawa, T. Nitta, H. Iida, *Org. Biomol. Chem.*, **2018**, *16*, 3999-4007.

[35] B. M. Maoz, Y. Chaikin, A. B. Tesler, O. Bar Elli, Z. Fan, A. O. Govorov, G. Markovich, *Nano Lett.* **2013**, *13*, 1203-1209.

Entry for the Table of Contents

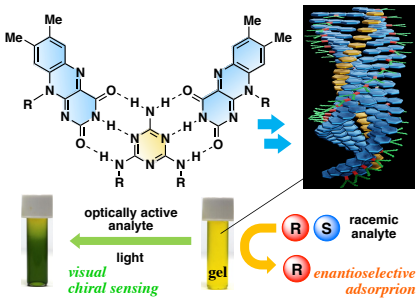

Hierarchical self-assembly of optically active riboflavin and melamine derivatives produces a chiral supramolecular organogel, which acts as a light-stimulated chiral sensor and a chiral adsorbent that enables colorimetric chiral discrimination and optical resolution.